A kinetic model of the co-operative binding of calcium and ADP to scallop (*Argopecten irradians*) heavy meromyosin

Miklós NYITRAI*†, Andrew G. SZENT-GYÖRGYI‡ and Michael A. GEEVES*[1]

*Department of Biosciences, University of Kent at Canterbury, Canterbury, Kent, CT2 7NJ, U.K., †Research Group for Fluorescence Spectroscopy, Office for Academy Research Groups Attached to Universities and Other Institutions, Department of Biophysics, Faculty of Medicine, University of Pécs, P.O.B. 99, H-7601 Pécs, Hungary, and ‡Rosenstiel Basic Medical Sciences Research Center, Brandeis University, Waltham, MA 02254-9110, U.S.A.

Analysis of the kinetics of ATP and ADP binding to scallop (*Argopecten irradians*) heavy meromyosin (HMM) showed that the only calcium-dependent process is the rate of ADP release. At physiological ionic strength calcium accelerated ADP release about 20-fold. Notably in the absence of calcium only one ADP bound HMM, with an affinity of 0.5–1 μM. The second nucleotide site remained unoccupied at up to 50 μM ADP yet could bind ATP rapidly. The calcium dependence of ADP-release rates showed that calcium binds co-operatively to scallop HMM with an affinity of 0.78 μM and a Hill coefficient of 1.9. Detailed interpretation of the data suggests that HMM exists in equilibrium between the on and off states and that calcium and ADP modulate the equilibrium between the two states. The on state is favoured in the presence of calcium and in the absence of both calcium and nucleotide. The off state is favoured by ADP (or ADP · P_i) in the absence of calcium. A detailed co-operative model of the interaction of ADP and calcium with HMM is presented.

Key words: ATPase activity, calcium regulation, enzyme kinetics, heavy meromyosin (HMM), myosin.

INTRODUCTION

Muscle contraction is initiated by a rise in the intracellular calcium concentration from its resting value (≈ 10 nM) to > 1 μM. The mechanism by which calcium activates a contraction varies with muscle type. In vertebrate skeletal muscle activation is brought about by calcium binding to the troponin complex of thin filaments [1]. In contrast, the activation of molluscan muscle is achieved by the direct binding of calcium to the essential light chain of myosin [2,3]. A related mechanism is found in vertebrate smooth muscle, which is activated by the phosphorylation of its regulatory light chain [4]. Myosin consists of two heavy and four light chains and is held together by a long C-terminal coiled-coil tail. The 100 kDa N-terminal globular motor domain of the heavy chain contains all of the actin-binding, ATPase and motor activity of the myosin. The motor domain is linked to the tail via a short helical neck which is stabilized by the light chains. While the double-headed heavy meromyosin (HMM) obtained by proteolytic fragmentation of vertebrate smooth-muscle and molluscan myosins preserve the regulatory mechanism, the single-headed myosin subfragment 1 (S1) is not regulated [5]. Full regulation appears to require the presence of an intact junction between the two heads formed by a stable coiled-coil region and may involve direct interactions between the two heads.

Structural studies have provided information regarding the molecular details of the mechanisms which are responsible for the regulation and function of the scallop (*Argopecten irradians*) myosin. The structure of the regulatory domain of scallop myosin was solved at 2.8 Å resolution [6] and the conformation of the scallop myosin head in its complex with nucleotides was also characterized [7,8]. However, the only structural model which has direct implications regarding the conformation of the scallop myosin in the low Mg^{2+}-ATPase activity form (referred to as the off state) is the low-resolution structure presented by Offer and Knight [9]. In this model the two heads of HMM from scallop striated muscle (scHMM) lie alongside one another with their bases in contact, and connections between the two heads are established through the regulatory light chains and between the regulatory light chain and the heavy-chain partner in the coiled coil. Interestingly, the three-dimensional structure of unphosphorylated smooth-muscle HMM (which is analogous to the calcium-free, i.e. off, state in scallop) involves asymmetric interactions between the two heads [10].

Significant information on the underlying mechanism of regulation of scHMM came from studies of the Ca^{2+} dependence of the ATPase reaction [11], which established that the ATPase was co-operatively activated by Ca^{2+}. A more recent study of the equilibrium binding of nucleotide and calcium to scHMM have extended our understanding of the co-operativity involved [5]. This work showed that calcium binding to the dimeric scHMM was co-operative in the presence of ADP but not in its absence. In contrast, ADP binding was tighter in the absence of calcium but was not co-operative. This suggests that co-operative switching of the HMM between two states (off and on) only occurs for calcium binding in the presence of ADP. In all other cases no co-operative switching is observed, i.e ADP binds to HMM non-co-operatively with a weaker affinity for the on state (presence of calcium) than the off state (no calcium). The co-operative binding of calcium in the presence of ADP is consistent with HMM · ADP being in the off conformation and is switched to the on conformation co-operatively by the binding of calcium.

Calcium also alters the sedimentation of HMM in the presence of ADP [12]. Co-operativity of calcium binding and calcium dependence of sedimentation can also be induced by ATP analogues in addition to ADP, suggesting that the off state, in

Abbreviations used: HMM, heavy meromyosin; scHMM, HMM from scallop striated muscle; S1, myosin subfragment 1; scS1, scallop S1; mant-ATP, 2′(3)-*O*-(*N*-methylanthraniloy)-ATP; mant-ADP, 2′(3)-*O*-(*N*-methylanthraniloy)-ADP; a.u., arbitrary units.

[1] To whom correspondence should be addressed (e-mail m.a.geeves@ukc.ac.uk).

contrast to the states of the contractile cycle, is less dependent on the particular nucleotide occupying the active site.

The kinetic characterization of events occurring during the ATP hydrolysis cycle is important in understanding the molecular mechanisms that underlie muscle contraction. The interaction of scHMM with nucleotides was characterized by transient kinetic methods more than 12 years ago using the intrinsic fluorescence from tryptophan residues in the protein and the fluorescent nucleotide analogue formycin triphosphate [12–14]. A more recent description [5] of the co-operative nature of calcium and nucleotide binding to HMM and the significant improvements in the optical-sensitivity transient kinetic equipment suggested that it was timely to re-examine these processes. The work is also a continuation of our recent study of the activity of S1 from different isoforms of scallop myosin to elucidate functional differences between the isoforms [15]. These kinetic studies provided a framework for the present investigations.

In the present work we studied the influence of calcium on the binding and dissociation of nucleotides to scHMM using stopped-flow methods to identify the Ca^{2+}-regulated kinetic steps. The results show that the kinetic behaviour of scHMM in the presence of calcium (the on state) is similar to that of scallop S1 (scS1), indicating that the two heads act independently. In the absence of calcium the ADP binds much more tightly to HMM but only one of the two heads of scHMM appears to be able to bind ADP, a result similar to recent studies of unphosphorylated smHMM [16]. Moreover in the absence of both calcium and ADP the population of scHMM is heterogeneous, with approximately one-third of the heads in the off conformation and the remaining number in the on conformation.

We propose here a regulatory model for the scHMM in which the protein exists in two conformations and nucleotide and calcium are allosteric effectors of the scHMM conformation. Calcium favours the on conformation whereas ADP favours the off state. The model can account for the co-operative binding of calcium to scHMM in the presence of ADP, which was observed previously for this type of myosin [5].

MATERIALS AND METHODS

HMM preparation and characterization

HMM was obtained from 4–5 g of striated scallop muscle myosin (*A. irradians*), which was prepared according to Stafford et al. [17]. Myosin ($\approx$ 15 mg/ml) dissolved in 0.5 M NaCl, 10 mM P_i, 10 mM Mops, 5 mM $MgCl_2$, 0.5 mM $CaCl_2$ and 0.5 mM dithiothreitol (pH 6.8) was digested for 2.5 min at 20 °C with tosylphenylalanylchloromethane ('TPCK')-treated trypsin (Sigma; 2.5 units/mg of myosin). The digestion was stopped by the addition of soya bean trypsin inhibitor at 10 mg/mg of trypsin and dialysed against 40 mM NaCl, 1 mM $MgCl_2$, 0.1 mM EDTA, 3 mM NaN_3, 0.5 mM dithiothreitol and 5 mM P_i, pH 7.0. The sample was clarified by 30 min of centrifugation at 100000 ***g***. To the supernatant 5 μM diadenosine pentaphosphate was added to inactivate possible adenylate kinase contamination. HMM was precipitated by adding 1.5 vol. of $(NH_4)_2SO_4$ solution saturated at 4 °C. The precipitate was redissolved in a small volume of 80 mM NaCl, 20 mM Mops, 2 mM $MgCl_2$, 0.1–1 mM EGTA, 3 mM NaN_3, 0.5 mM dithiothreitol and 0.2–0.5 mM ADP, pH 6.8 (ADP and dithiothreitol protects HMM from inactivation and aggregation). Trypsin inhibitor was removed by Sephadex G-100 gel filtration on a 2.6 cm $\times$ 90 cm column. Fractions (2.5 ml) were collected with a flow rate of 0.5–1 ml/min. Fractions in excess of 1 mg/ml were combined, concentrated by $(NH_4)_2SO_4$ precipitation between 48 and 60 % $(NH_4)_2SO_4$ saturation [at a $(NH_4)_2SO_4$ saturation of 48 % HMM of lower activity and calcium sensitivity is caused to precipitate]. The precipitate was dialysed against the column buffer and stored in liquid nitrogen. Activity and calcium sensitivity were retained, provided that thawing was rapid by placing the vial in a 20 °C water bath for 5 min. Proteolysis of the motor domain was limited by the short tryptic digestion used. Two species of HMM were produced, differing in tail length by 20–23 nm [18].

The scHMM was routinely checked by measuring its Mg^{2+}-ATPase activity in the absence of actin and the calcium sensitivity of the activity using the coupled-assay method [5]. The turnover rate/scHMM head was in the range of 0.32–0.36 s^{-1} in the presence of calcium; the calcium sensitivity $[(ATPase^{+Ca} - ATPase^{-Ca}) \times 100/ATPase^{+Ca}]$ of the preparations was between 85 and 92 %.

Kinetic experiments

All experiments were carried out at 20 °C in a standard buffer of 20 mM Mops, pH 7.0, 100 mM KCl, 5 mM $MgCl_2$ and either 100 μM EGTA or 100 μM $CaCl_2$, unless stated otherwise. When measurements were recorded as a function of *p*Ca the calcium concentration was buffered by the addition of appropriate amounts of 2 mM EGTA and 2 mM Ca-EGTA [19]. Fluorescence transients were recorded with a standard Hi-Tech SF-61DX2 stopped-flow spectrophotometer (Hi-Tech, Salisbury, Wilts, U.K.). Fluorescence was excited at 295 nm (tryptophan) or 365 nm [mant nucleotides; 2′(3)-*O*-(*N*-methylanthraniloy)-ATP (mant-ATP) and 2′(3)-*O*-(*N*-methylanthraniloy)-ADP (mant-ADP)], using a 75 W Xe/Hg lamp and monochromator. Fluorescence emission was monitored through WG320 or KV389 cut-off filters in the case of experiments with tryptophan and mant fluorescence, respectively. All the transients shown are the average of between three and six shots of the stopped-flow apparatus. The concentrations used to describe the experimental conditions are those established after mixing the reactants in the stopped-flow apparatus (dilution by 2, 1:1 mixing), unless specified otherwise.

Stock scHMM was routinely stored with ADP present. Dilution of the stock protein into experimental buffers normally reduced the ADP to insignificant levels. This was confirmed by pretreating the samples with apyrase.

Interpretation of the kinetic data

The kinetic parameters obtained were interpreted in terms of the seven-step Bagshaw–Trentham mechanism of the myosin ATPase (Scheme 1) [20]. In the model k_{+i}, k_{-i} and K_i (defined as k_{+i}/k_{-i}) are the forward and reverse rate constants and the forward equilibrium constant of the *i*th step of the reaction, respectively. In Scheme 1 asterisks refer to a different conformational state of the protein, reflected by a change in protein fluorescence. In this scheme nucleotide binding is assumed to be a two-step process, a rapid equilibrium step (Scheme 1, reactions 1 and 7) followed by a slower conformational change (Scheme 1, reactions 2 and 6). The dissociation constant for ADP is defined as K_6K_7 and can be estimated either from the ratio of dissociation (k_{+6}) and association (k_{-6}/K_7) rate constants ($k_{+6}K_7/k_{-6}$) or from the amplitudes of the fluorescence changes observed on adding nucleotide, which are proportional to the fraction of HMM-binding nucleotide.

In a stopped-flow experiment the amplitude (A) of the fluorescence change can be defined from the observed transients as:

$$A = (F_{t-\infty} - F_{t-0})/F_{t-0} \quad (1)$$

where F_{t-0} is the fluorescence of the free fluorophore or protein and $F_{t-\infty}$ is the fluorescence at equilibrium. In ADP-binding

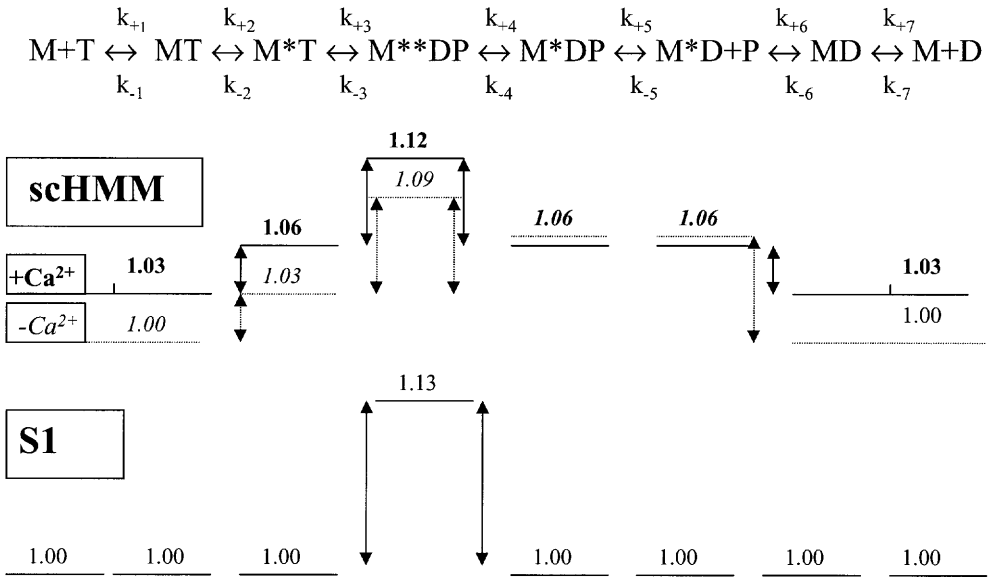

Scheme 1 Seven-step kinetic scheme for the interaction of myosin with nucleotides [20]

In the model the forward (k_{+i}) and reverse (k_{-i}) rate constants are presented. Below the Scheme the changes in tryptophan fluorescence attributed to the individual steps are shown. The numbers give the fluorescence intensities relative to that for the nucleotide-free scHMM in the absence of calcium. For comparison the values for scS1 are also shown, from [15]. M, myosin; D, ADP; P, inorganic phosphate; T, ATP.

experiments the fractional amplitude of tryptophan fluorescence was directly proportional to [M*D] and in all cases ADP was in great excess over scHMM ([D] $\gg$ $[M]_{total}$). The measured amplitudes were analysed to obtain dissociation equilibrium constants by fitting the following equation:

$$A = A_{max}[D]/(K_D + [D]) \quad (2)$$

where A_{max} is the fluorescence amplitude at saturating [ADP]. In mant-ADP-binding experiments the fluorescence quantum yields of the bound and free mant nucleotide are φ_{free} and φ_{bound}, respectively, and the following equations apply:

$$F_{t=0} = [mant]_{total} \times \varphi_{free} \quad (3)$$

$$F_{t=\infty} = [mant]_{bound} \times \varphi_{bound} + ([mant]_{total} - [mant]_{bound}) \times \varphi_{free} \quad (4)$$

where $[mant]_{total}$ refers to the total concentration of mant nucleotides in solution and $[mant]_{bound}$ to the fraction of mant nucleotides bound to myosin. By combining eqns (1), (3) and (4):

$$A_{corr} = A \times [mant]_{total} = [mant]_{bound} \times (\varphi_{bound} - \varphi_{free})/\varphi_{free} \quad (5)$$

Therefore, $A \times [mant]_{total}$ is directly proportional to the concentration of the bound mant nucleotide and the corrected values [A_{corr}; in arbitrary units (a.u.)] are presented throughout the paper.

RESULTS

The effect of calcium on the Mg^{2+}-ATPase activity of scHMM

Mg^{2+}-ATPase activity of scHMM was measured with the coupled assay (see the Materials and methods section) in the presence and absence of calcium. The calcium sensitivity of the three independent preparations used here was between 85 and 92%. The fraction of scHMM that is regulated and the effect of calcium on the ATPase activity of scHMM can be estimated more directly using the single turnover assay introduced by Jackson and Bagshaw [14]. scHMM (0.5 μM) was mixed in a double-mixing stopped-flow apparatus with 5 μM mant-ATP and aged for 1 s to allow complete binding of mant-ATP to the protein. The reactants were then mixed with a large excess of ATP (400 μM) to displace the bound mant nucleotide. In the presence of calcium a single exponential decrease in fluorescence was observed with a k_{obs} value of 0.33–0.38 s^{-1}, in close agreement with the results of steady-state ATPase assays (0.32–0.36 s^{-1}; see the Materials and methods section). In the absence of calcium a double exponential decay of fluorescence was observed. The faster component had a k_{obs} of 0.35–0.6 s^{-1}, similar to that obtained in the presence of calcium, and was followed by a slower component with a k_{obs} of 0.0036–0.0072 s^{-1}. This slower component represented the regulated scHMM population. The ratio of the fluorescence amplitudes measured in the faster and slower phases was 1:5. These results suggest that the ATPase activity of the regulated heads is activated by 50–100-fold upon calcium binding, a conclusion that is in agreement with previous data [12,14,21,22]. The ratio of these amplitudes suggests that approx. 16–17% of the heads were unregulated, i.e. were not turned off by the removal of calcium, consistent with the results of the steady-state ATPase measurements.

The binding of ATP or mant-ATP to scHMM

scHMM (0.5 μM) was reacted with excess ATP at concentrations ranging from 5 to 1000 μM in the presence or absence of calcium. Figure 1(a) shows the increase in tryptophan fluorescence on binding 5 and 20 μM ATP in the absence of Ca^{2+}. The fluorescence increased by 9% and was well described by a single exponential function. The dependence of the observed rate constant (k_{obs}) and the amplitude on [ATP] are shown in Figure 1(b) for experiments in the presence and absence of calcium. The k_{obs} and amplitude data were identical in the presence and absence of Ca^{2+} (Figure 1b and Table 1).

The k_{obs} determined from the fluorescence traces was dependent in a linear fashion on the ATP concentration below 20 μM. Above this concentration range the slope of the linear fit to the k_{obs} versus ATP curves gave second-order rate constants of 4×10^6 $M^{-1} \cdot s^{-1}$ ($K_1 k_{+2}$ in Scheme 1). The ATP dependence of k_{obs} was hyperbolic when studied over greater ATP concentrations (Figure 1b). Hyperbolae fits resolved a k_{max} value of 320 ± 20 s^{-1}, whereas half saturation was obtained at 80 μM ATP. The maximum value of k_{obs} corresponds to $k_{+3} + k_{-3}$ in Scheme 1. It is notable that the amplitudes of the fluorescence transients decreased from 9 % at low [ATP] values to 3 % at high [ATP] values after correcting for losses in the dead time. This is similar to the results observed for mammalian skeletal-muscle S1 and has been attributed to the loss (in the mixing time) of the fluorescence change occurring on the formation of M*T (Scheme 1), leaving only the signal change on the hydrolysis step ($k_{+3} + k_{-3}$) [23,24]. However, this loss of signal was not observed earlier for scS1 [15]. This was rationalized by the observation that the loss of amplitude is normally only seen for myosin heads, which contain an additional tryptophan near the nucleotide-binding pocket, but not for myosins lacking such residues (e.g. *Dictyostelium* myosin II S1, smooth-muscle myosin S1 and scS1). Thus the total fluorescence signal has two components. The first originates from nucleotide binding and the k_{obs} is related linearly to the concentration of ATP. This process is very fast at high concentrations of ATP and so is lost in the dead time of the instrument [23]. The second component originates from the slower ATP-hydrolysis step and is always observed. More recent analysis using single-tryptophan mutants of *Dictyostelium* S1 suggests that the fluorescence changes from any individual tryptophan may be complex [25]. However, the observation that we see a loss of fluorescence amplitude at high [ATP] values for scHMM but not for scS1 may indicate that there are additional conformational changes occurring in scHMM.

When mant-ATP bound to scHMM the fluorescence intensity of the mant signal increased. The corrected amplitude of the fluorescence change was calcium-independent ($A_{corr} = 1.0$–1.2 a.u.) and mant-ATP-independent in the concentration range 5–20 μM. The k_{obs} increased linearly with mant-ATP concentration over the same range and the slope of the linear fit gave a calcium-independent second-order rate constant ($K_1 k_{+2}$) of 3.5×10^6 $M^{-1} \cdot s^{-1}$. The intercept values from the plots were very small compared with the range of measured k_{obs} values and thus their proper determination was not possible, as in the case of ATP.

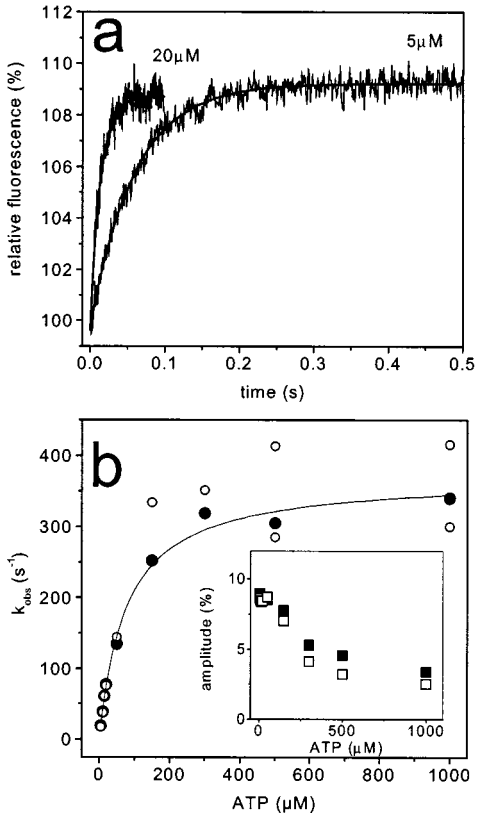

Figure 1 Transient changes in tryptophan fluorescence induced by the binding of ATP to scHMM

scHMM (0.5 μM) was mixed with excess ATP in the presence or absence of calcium. (**a**) Transients observed in the absence of Ca^{2+} with the best-fit single exponential function superimposed. (**b**) The k_{obs} values as a function of [ATP] in the presence (●) and absence (○) of Ca^{2+}. The best-fit hyperbola is superimposed and defines $k_{max} = 320 \pm 20$ s^{-1} with half-saturation at 80 μM ATP. The insert shows the [ATP] dependence of the measured amplitude (symbols in the insert mean the same as in the main panel).

The binding of ADP to scHMM

scHMM (0.5 μM) was mixed with ADP at concentrations of between 5 and 1000 μM. The binding of ADP to scHMM resulted in an increase in tryptophan fluorescence. Figure 2 shows the fluorescence changes on binding 5 and 100 μM ADP in the presence and absence of calcium. The amplitude and the k_{obs} values of the changes are presented in Figure 2(c) and are calcium-dependent. The ADP dependence of the fluorescence amplitudes was hyperbolic and fits to these curves gave a maximum amplitude value of ≈ 3 % with half-saturation at 10 ± 1 μM in the presence of calcium. The half-saturation ADP concentration provides an estimate of the equilibrium dissociation constant for ADP binding ($K_6 K_7$ in Scheme 1). In the absence of calcium the maximum amplitude and half-saturation values were 6–7 % and 3 ± 1 μM ADP respectively. The ADP dependence of the k_{obs} values appeared to be linear below 50 μM. The fits resulted in calcium-independent second-order rate constants of $(1 \pm 0.2) \times 10^6$ $M^{-1} \cdot s^{-1}$ (k_{-6}/K_7 from Scheme 1) with intercept values of 0.8 ± 0.6 s^{-1} and 20 ± 10 s^{-1} in the absence and presence of calcium, respectively. The intercept values correspond to the rate constant characteristic for the dissociation of ADP from the scHMM (k_{+6} in Scheme 1). When analysed at higher ADP concentrations (up to 1000 μM ADP), the k_{obs}-versus-[ADP] curves were fitted with hyperbolae (Figure 2c). Half-saturation occurred at 200 ± 20 μM ADP, independent of the presence of calcium. The k_{max} values ($k_{+6} + k_{-6}$ in Scheme 1) were 205 ± 17 s^{-1} and 190 ± 5 s^{-1}, whereas k_{+6} was determined to be 20 ± 9 s^{-1} and 0.6 ± 0.3 s^{-1} in the presence and absence of calcium, respectively. Therefore, k_{-6} was calcium-independent with a value of 180–190 s^{-1}.

Displacement of ADP by excess ATP

To measure k_{+6} directly scHMM (0.5 μM) was mixed with 400 μM ATP in either the absence of ADP or in its presence by incubating the scHMM with ADP before the shots. Figure 3 shows the tryptophan fluorescence measured in the presence (Figure 3a) or absence (Figure 3b) of calcium. In the absence of ADP the transients were single exponential and calcium-independent and gave a k_{obs} value of 310 ± 10 s^{-1}. In the presence of calcium and 120 μM ADP (providing ≈ 90 % saturation in ADP if $K_6 K_7 = 15$ μM) only a slow process was present with a k_{obs} of 18 ± 3 s^{-1} (Figure 3a). The value of k_{obs} was independent

Table 1 Rate and equilibrium constants for the interaction of scHMM with nucleotides

Nomenclature is used according to Scheme 1 [20]. scS1 data are from [15]. Data for ATP are from ATP-binding experiments (Figure 1). ND, not determined.

			Value		
Ligand	Parameter	Units	$+Ca^{2+}$	$-Ca^{2+}$	scS1
ATP	K_1k_{+2}	$10^6\ M^{-1}\cdot s^{-1}$	4.0	4.0	3.9
	K_1	10^{-6} M	80	80	390
	$k_{+3}+k_{-3}$	s^{-1}	320	320	ND
mant-ATP	K_1k_{+2}	$10^6\ M^{-1}\cdot s^{-1}$	3.5	3.5	5.9
ADP	k_{-6}/K_7*	$10^6\ M^{-1}\cdot s^{-1}$	1	1	ND
	k_{+6}†	s^{-1}	15	0.8	18.5
	k_{-6}‡	s^{-1}	190	190	ND
	K_7‡	10^{-6} M	200	200	ND
	K_6K_7§	10^{-6} M	15	0.8	9.8
mant-ADP	k_{-6}/K_7¶	$10^6\ M^{-1}\cdot s^{-1}$	1	0.5–0.8	1.5
	k_{+6} ‖	s^{-1}	15	0.3–0.7	17
	K_6K_7§	10^{-6} M	15	1	11

* From ADP-binding experiments (Figure 2).

† From ADP displacement with ATP (Figure 3) and intercepts (Figure 2).

‡ From Figure 2.

§ Data calculated using the dissociation (k_{+6}) and association ($k_{-6}K_7$) rate constants and compatible amplitudes analysis in Figures 2(b), 3(c), 3(d) and 4(c).

¶ From Figure 4.

‖ From intercepts of linear fits in mant-ADP-binding experiments (Figure 4) or from mant-ADP displacement with ATP (Figure 5).

of increases in either [ADP] or [ATP]. In the absence of calcium at 25 μM ADP (more than 90 % saturation if $K_6K_7 = 1\ \mu$M) the amplitude of the fast phase decreased to approximately half of its value measured in the absence of ADP. The amplitude of the slow phase was very small and at 25 μM ADP approx. 1 % of the F_{t-0}.

To gain further information scHMM (0.5 μM) was incubated with a range of ADP concentrations and then mixed with 400 μM ATP. The k_{obs} value attributed to the faster phase remained calcium- and ADP-independent and ranged between 280 and 350 s^{-1}. Figures 3(c) and 3(d) show the ADP dependence of the measured amplitudes. Note that in this case the ADP concentrations are plotted as adjusted before the stopped-flow shots since the equilibrium binding of ADP was established before the mixing. In the presence of calcium the amplitude of the fast phase decreased from 6.7 % to zero and the slow phase increased from zero to 5.3 % as the ADP concentration increased (Figure 3c). The k_{obs} for the slow phase was ADP-independent and gave a k_{obs} of $15\pm4\ s^{-1}$ (k_{+6}). In this experiment the fast phase represented scHMM sites with no bound ADP, to which ATP binds quickly. The slow phase represented scHMM heads with a bound ADP in the nucleotide pocket, which must dissociate before ATP can bind. Analysis of the two phases independently gave an ADP affinity of $15\pm3\ \mu$M consistent with the rate and amplitude measurements for ADP binding in Figure 2. Since at the concentrations used here ATP and ADP bind with fluorescence increases of 8–9 and 3 % respectively (Figures 1 and 2) the maximum slow-phase amplitude reflects the difference between these values.

In the absence of calcium the amplitude of the faster phase decreased as the ADP concentration increased but to only 45 % of that value measured in the absence of ADP (Figure 3d). This observation indicates that about half of the scHMM heads did not bind ADP over this concentration range. The hyperbolic fit

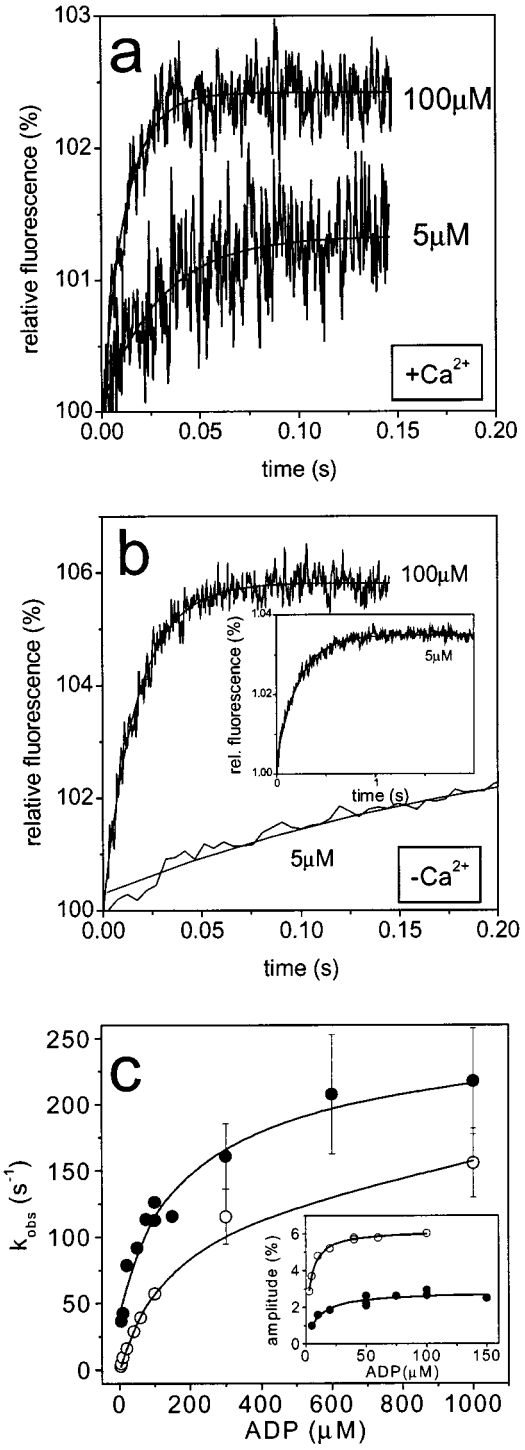

Figure 2 Transient changes in tryptophan fluorescence induced by the binding of ADP to scHMM

Fluorescence transients recorded on mixing 0.5 μM scHMM with excess ADP in the presence (**a**) and absence (**b**) of calcium. Single exponential fits are shown superimposed. The insert in (**b**) shows the full transient for 5 μM ADP in the absence of calcium. (**c**) The k_{obs} values in the presence (●) and absence (○) of Ca^{2+}. Fitted values for the hyperbolae are quoted in the text and in Table 1. The insert in (**c**) shows the ADP dependence of the measured amplitudes, which defines the dissociation equilibrium constants (K_D) for ADP as 3 μM ($-Ca^{2+}$) and 10 μM ($+Ca^{2+}$).

to the amplitude of the fast phase gave a half-saturation value (K_6K_7) of $1.7\pm0.3\ \mu$M (Figure 3d), again consistent with the ADP-binding data of Figure 2. Reliable fits to the amplitude of

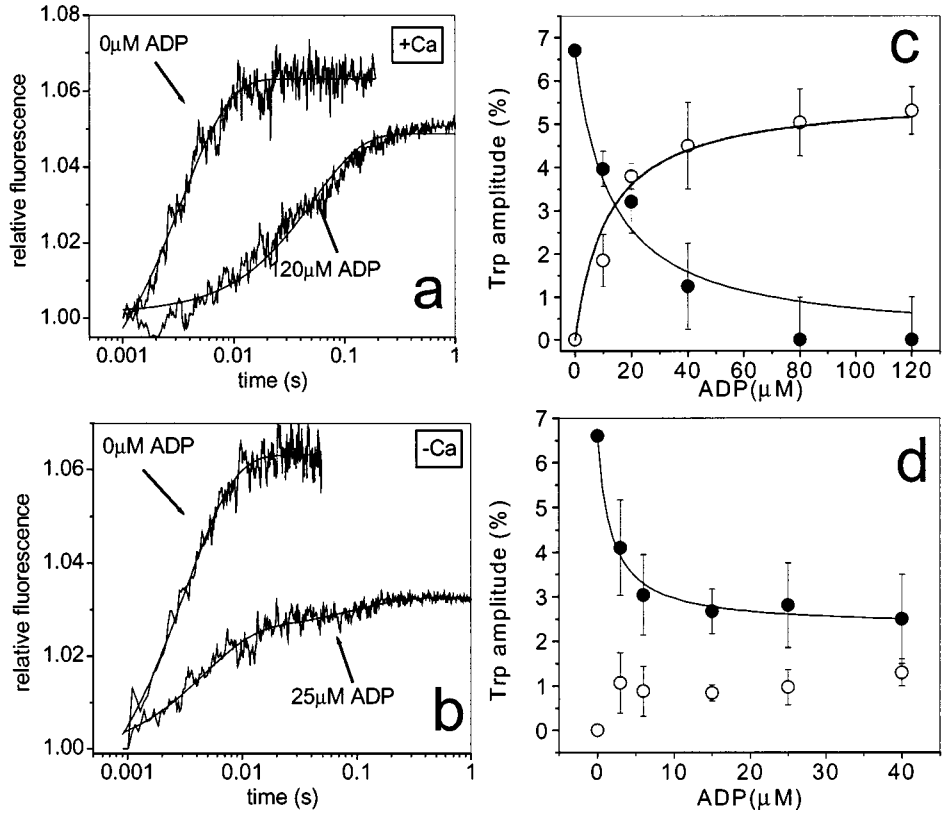

Figure 3 Displacement of ADP from scHMM by excess ATP

The tryptophan fluorescence transients recorded on mixing 400 μM ATP with 0.5 μM scHMM pre-equilibrated with ADP (as indicated) in the presence (**a**) or absence (**b**) of calcium. In absence of ADP the transients were fitted with a single exponential function (k_{obs}, 310 ± 10 s^{-1} with or without calcium; see Figure 1). In the presence of ADP a second slower phase appeared. (**a**) In the presence of calcium at high [ADP] (120 μM) only the slow phase was seen with $k_{obs} = 18.9$ s^{-1} and an amplitude of 4.8%. (**b**) Shows the transient measured in the presence of 25 μM ADP with the double exponential fit, which resulted in k_{obs} values and amplitudes of 280 and 10 s^{-1} and 2.7 and 0.7% for the fast and slow phases, respectively. (**c**) The [ADP] dependence of the amplitudes of the faster (●) and slower (○) phases in the presence of calcium. Note that the [ADP] is quoted before 1:1 mixing. The hyperbolae fitted to either amplitudes gave a dissociation equilibrium constant (K_D) for ADP of 15 ± 3 μM. (**d**) As for (**c**) but in the absence of calcium. The fit to the faster-phase amplitude resulted in a K_D of 1.7 ± 0.3 μM in the absence of calcium. Note that the amplitude of the faster phase does not disappear at high [ADP].

the slow phase were not possible as the value of this parameter remained small (1%) even at higher ADP concentrations. This is predicted from the nucleotide-binding experiments, where the fluorescence changes upon ADP (6–7%) and ATP (8–9%) association were found to be similar. The k_{obs} for the slower phase where it could be measured was 5–15 s^{-1}, which is similar to that measured in the presence of calcium (15 ± 4 s^{-1}). This probably reflects the contribution of the 10–15% unregulated heads to the measured fluorescence signal in our experiments. The determination of the rate constant of ADP dissociation from scHMM in the absence of calcium is not possible from these tryptophan fluorescence data. Nevertheless, the observation that approximately half of the scHMM heads were unable to bind ADP in the absence of calcium remained clear.

The binding of mant-ADP to scHMM

scHMM (0.5 μM) was mixed with various concentrations (2–20 μM) of mant-ADP in the presence or absence of calcium. The fluorescence of the mant-ADP increased upon binding to scHMM (Figure 4a) and in the presence of calcium the fluorescence transients were well described by single exponential functions. Linear fit to k_{obs}-versus-[mant-ADP] curves (Figure 4b) gave a second-order rate constant of 1.0×10^6 M$^{-1} \cdot$ s^{-1} (k_{-6}/K_7) and the intercept value was 13 ± 3 s^{-1} (k_{+6}). The mant-ADP dependence of the amplitudes fitted to a hyperbola resulted in a half-saturation concentration of 16 μM (K_6K_7 in Scheme 1) and maximum amplitude value of $A_{corr} = 0.9$ a.u. in the presence of calcium (Figure 4c). These rate and equilibrium constants are all very similar to those estimated for ADP.

The transients obtained in the absence of calcium consisted of two phases (Figure 4a) and were fitted to a two-exponential function (Figure 4b). A linear fit to the two sets of k_{obs} values plotted against the mant-ADP concentration gave lines with similar gradients [apparent second-order rate constants of $(0.5–0.8) \times 10^6$ M$^{-1} \cdot$ s^{-1}] but different intercepts. For the faster component the intercept value was 14 ± 2 s^{-1} and 0.8 ± 0.3 s^{-1} was found for the slower component. These values were almost the same as those in ADP-binding experiments in the presence and absence of calcium and suggest the presence of two scHMM components. Fitting hyperbolae to the mant-ADP dependence of the amplitudes of the two components gave half-saturation values (K_6K_7) of 15 ± 2 and 2.5 ± 1.0 μM and maximum corrected amplitudes (A_{corr}) of 0.7 and 0.2 a.u. for the faster and slower components, respectively (Figure 4c). The fast component is almost identical to that found in the presence of calcium yet the amplitude is much greater than expected for the unregulated fraction of scHMM (10–20%). This suggests that even in the

absence of calcium a significant fraction of the HMM binds mant-ADP as though it had calcium bound to it. This issue will be considered further in the Discussion.

Dissociation of mant-ADP by excess ATP

In mant-ADP-displacement experiments scHMM (0.5 μM) was equilibrated first with mant-ADP (20 μM) and then mixed with a large excess of ATP (400 μM). The fluorescence intensity of mant-ADP decreased during the measurements, which indicated that the fluorescent nucleotide dissociated from the protein. The use of excess ADP instead of ATP as a displacing agent or apyrase (5 units/ml) to chase the mant-ADP did not influence the observed transients in control experiments.

When the transient was recorded in the presence of 100 μM free calcium the traces could be described by a single exponential function and the observed rate constant was 15 s^{-1}. The corrected relative amplitude (A_{corr}) was determined to be 0.4–0.5 a.u. In the absence of calcium a single exponential fit gave the k_{obs} value of 0.7 ± 0.1 s^{-1} with an amplitude of about $A_{corr} = 0.6$ a.u. However, in this case the fit with two exponential components proved to be better. The component resolved with a larger amplitude could be characterized with a k_{obs} of 0.3–0.6 s^{-1} similar to that in single exponential fits. The other, faster component had a k_{obs} value ranging between 10 and 15 s^{-1}, similar to that seen in the presence of calcium. The contribution of the faster component to the total fluorescence change was 10–20 %. The faster component therefore probably represents the unregulated fraction of the scHMM in the sample.

These data show that the rate constant characteristic for the dissociation of mant-ADP from scHMM is 15 s^{-1} in the presence of calcium and 0.3–0.7 s^{-1} in the absence of calcium. These values are compatible with the estimates of k_{+6} from the intercepts of Figure 4 and similar to the values for ADP.

The substantial difference between the mant-ADP-displacement values obtained in the presence and absence of calcium provided an experimental tool to measure the calcium dependence of k_{+6}. In these experiments mant-ADP was displaced by excess ATP in the presence of different free calcium concentrations. Figure 5(a) shows the *p*Ca dependence of the fluorescence transients and Figure 5(b) shows the [Ca^{2+}] dependence of the k_{obs} values characteristic for the major component of the fluorescence decay, which showed a steep increase between 0.1 and 1 μM free calcium. Fitting the data to the Hill equation showed that k_{obs} changed between its extreme values of 0.3 and 15 s^{-1} with half-saturation achieved at 0.78 ± 0.03 μM free calcium and a Hill coefficient of 1.9 ± 0.1. These values are in good agreement with values from steady-state measurements [5]. A fast component appeared below 1 μM calcium with a k_{obs} value between 3 and 14 s^{-1}. This component was attributed to the unregulated scHMM fraction.

The kinetics of the regulatory conformational change

In the absence of nucleotides the binding of calcium to scHMM produces a 3 % increase in protein fluorescence intensity and thus a direct measure of the calcium-induced change in tryptophan fluorescence was possible, as reported by Jackson and Bagshaw [12]. At 10 μM calcium the binding of calcium was very fast and the rate constant characteristic for this event could not be resolved in our experiments. When 0.5 μM scHMM and 10 μM Ca^{2+} were mixed with 500 μM EGTA the fluorescence intensity of tryptophan decreased by 3 % (Figure 6a). The k_{obs} characteristic for this fluorescence change was found to be 70 s^{-1}.

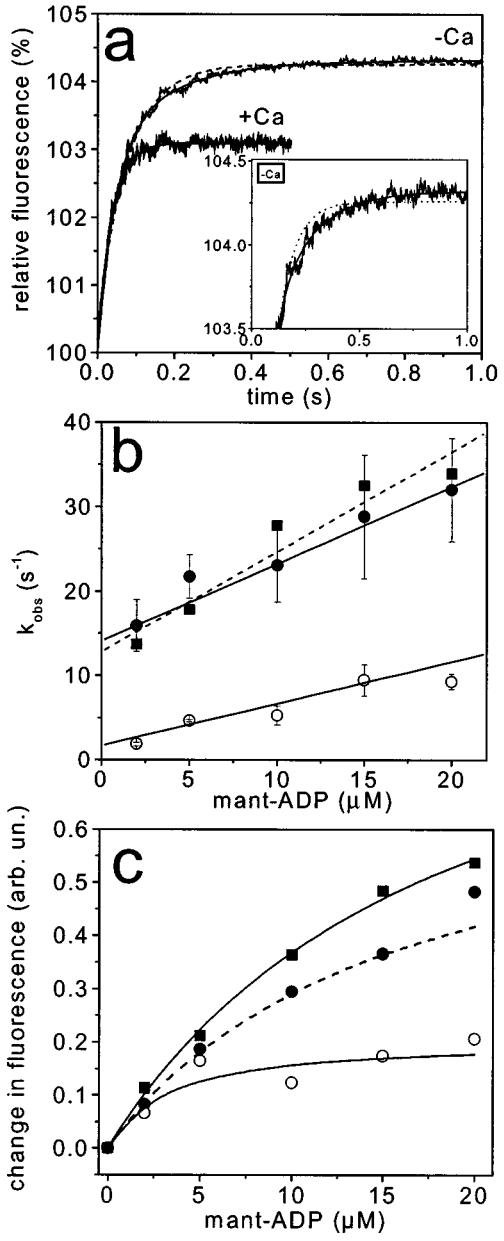

Figure 4 Transient changes in mant fluorescence induced by the binding of mant-ADP to scHMM

(**a**) Fluorescence transients observed on mixing 0.5 μM scHMM with 10 μM mant-ADP in the presence and absence of calcium with the best fit to single ($+Ca^{2+}$) or double exponential ($-Ca^{2+}$) functions superimposed. The dashed line in the insert is a single exponential fit to the $-Ca^{2+}$ data for comparison. (**b**) The [mant-ADP] dependence of k_{obs} in the absence (●, measured for the fast fluorescence transient component; ○, slow component) and presence (■) of calcium. Linear fits resulted in second-order rate constants of 1.0×10^6 $M^{-1} \cdot s^{-1}$ and an intercept value of 13 ± 3 s^{-1} in the presence of calcium (dashed line). In the absence of calcium the second-order rate constants was $(0.5–0.8) \times 10^6$ $M^{-1} \cdot s^{-1}$ for both phases. The intercepts were 14 ± 2 and 0.8 ± 0.3 s^{-1}. (**c**) Shows the corresponding amplitudes using the same symbols. Solid lines show the hyperbolic fits, which gave dissociation equilibrium constant (K_D) values for mant-ADP of 16 μM in the presence of calcium (■) and of 15 μM (●) and 2.5 μM (○) in the absence of calcium. Extrapolation to saturating [mant-ADP] gave a maximum amplitude of 0.9 a.u. in the presence of calcium and of 0.7 and 0.2 a.u. for the fast and slow phases, respectively, in the absence of calcium.

The Ca^{2+}-induced conformational changes preceded nucleotide binding. This was shown by Ca^{2+}-jump measurements in the presence of ADP or mant-ADP. scHMM (0.5 μM), 10 μM Ca^{2+}

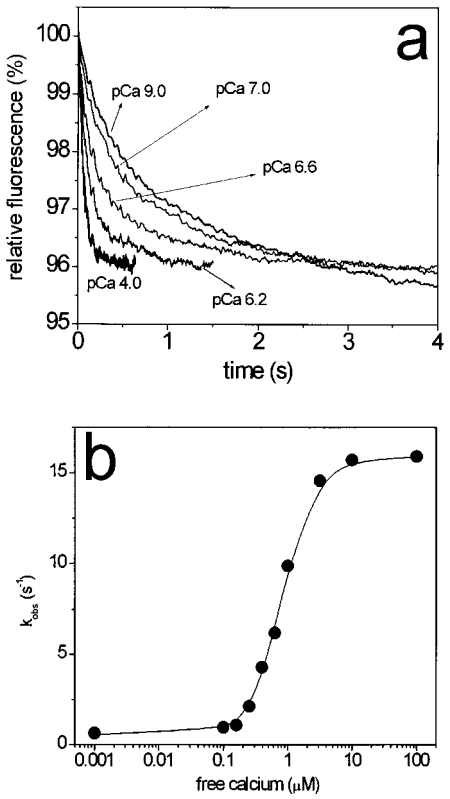

Figure 5 The displacement of mant-ADP from scHMM with excess of ATP

(**a**) scHMM (0.5 μM) and 40 μM mant-ADP was mixed with 400 μM ATP. Fluorescence transients were recorded as a function of free calcium concentration (pCa 4.0, 6.2, 6.6, 7.0 and 9.0). (**b**) The k_{obs} values as a function of free calcium concentration. Solid line represents the result of fit obtained from Hill analysis. Half-saturation at [Ca^{2+}] of 0.78 ± 0.03 μM with a Hill coefficient of 1.9 ± 0.1.

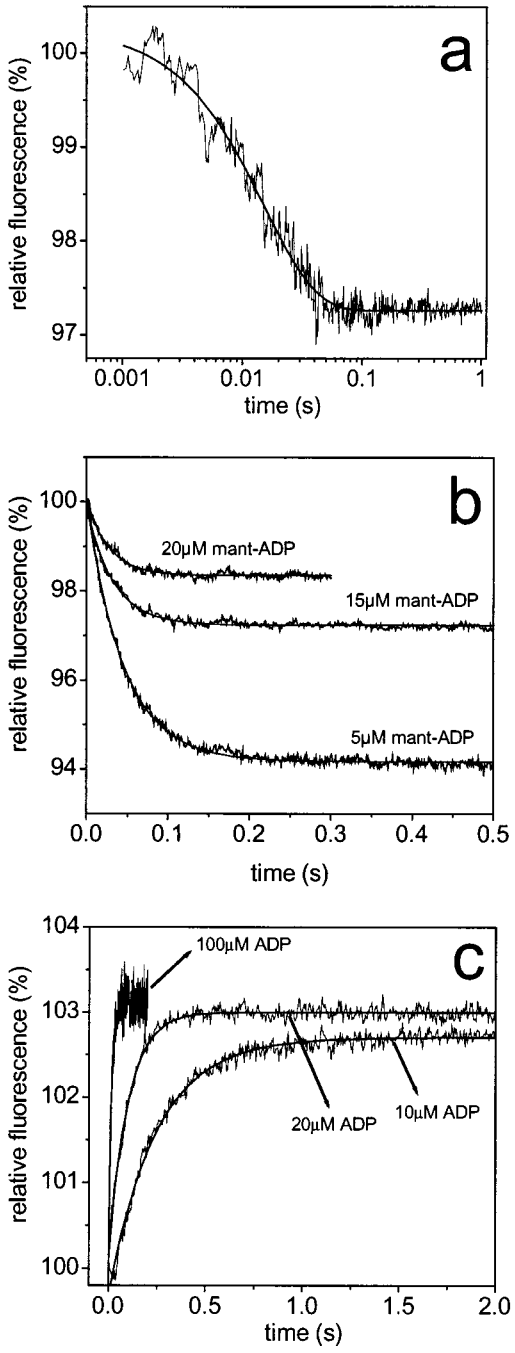

Figure 6 Transient fluorescence changes induced by the dissociation or binding of calcium to scHMM

(**a**) The change in protein fluorescence was recorded when 0.5 μM scHMM and 10 μM calcium was mixed with 500 μM EGTA. Solid line represents the single exponential fit. The k_{obs} was 70 s^{-1} and the amplitude of the change in tryptophan fluorescence was 3%. (**b**) Mant fluorescence transients from experiments where 0.5 μM scHMM and 50 μM EGTA and mant-ADP at different concentrations (as indicated) were mixed with 500 μM calcium. Single exponential fits (superimposed as solid lines) resolved k_{obs} values of 21.7, 30.5 and 35.6 s^{-1} with amplitudes of 5.8, 2.6 and 1.6% at 5, 15 and 20 μM mant-ADP, respectively. (**c**) Tryptophan fluorescence transients observed when 0.5 μM scHMM and 10 μM calcium and various ADP concentrations (as indicated) were mixed with 500 μM EGTA. Single exponential analyses gave k_{obs} values of 4.1, 10.1 and 71.5 s^{-1} with amplitudes of 2.7, 3.0 and 3.1% at 10, 20 and 100 μM ADP, respectively.

and various concentrations (5–20 μM, the concentration after mixing was completed) of mant-ADP were mixed with 500 μM EGTA. The fluorescence intensity of mant increased, compatible with the removal of calcium resulting in net binding of mant-ADP at this concentration due to the higher mant-ADP affinity in the absence of calcium. The fluorescence transient could be described by a single exponential function and the k_{obs} values were in good agreement with those obtained when scHMM was reacted with mant-ADP in the absence of calcium. Thus the calcium equilibrates on scHMM much faster than the mant-ADP. The reverse reaction showed a similar result (Figure 6b). Thus when 0.5 μM scHMM in 50 μM EGTA and various concentrations (5–20 μM) of mant-ADP were mixed with 500 μM Ca^{2+} the mant fluorescence decreased, compatible with mant-ADP dissociation. The traces were well fitted with a single exponential function and k_{obs} values were identical to those measured for mant-ADP-binding experiments in the presence of calcium. The amplitudes measured in all of these mant-ADP experiments corresponded to the mant fluorescence differences detected between mant-ADP–scHMM complexes in the absence and presence of calcium. These results are consistent with the equilibration of calcium being faster than ADP equilibration and the only reaction observed is ADP binding and release at the rate expected after equilibration with calcium.

In another set of experiments the mant-ADP–HMM was mixed with ATP at the same time as jumping the calcium concentration. These measured the rate of mant-ADP displacement and the k_{obs} were again consistent with rapid calcium equilibration followed by mant-ADP release.

The calcium-jump experiments in the presence of mant-ADP were restricted to a maximum of 20 μM mant-ADP because of the background mant fluorescence. A higher concentration range (10–500 μM) is possible when monitoring tryptophan fluorescence and using ADP. When the scHMM and ADP were mixed with EGTA the tryptophan fluorescence intensity increased for all ADP concentrations by about 3 % (Figure 6c), consistent with the difference between the fluorescence amplitudes measured when scHMM was mixed with ADP in the presence and absence of calcium (see Scheme 1). The k_{obs} values determined from single exponential fits were identical to those for ADP-binding measurements in the absence of calcium at an equivalent ADP concentration (Figure 2b). This suggests that even at 500 μM ADP the calcium equilibrates faster than ADP and furthermore even though the HMM is saturated with ADP both in the presence and absence of calcium we observed a transient consistent with 50 % of the ADP dissociating from the complex.

For all of the results obtained during the Ca-jump experiments the measured kinetic parameters were characteristic of the conformation of scHMM that was established after the stopped-flow shot was completed. Accordingly, the calcium-induced conformational changes in scHMM occurred faster than the binding or dissociation of nucleotides. Under the experimental conditions used here the k_{obs} values were up to 150 s^{-1}. These experiments, therefore, provided an upper limit of approx. 6–7 ms for the time period within which the calcium-induced conformational change was completed.

DISCUSSION

The work presented here is summarized in Table 1 together with the kinetic data for scS1 reported by Kurzawa-Goertz et al. [15]. Almost all of the data for scS1 are similar to the data for scHMM in the presence of calcium. The only exception to this was that we were able to define the maximum rate of change of fluorescence on binding ATP (320 s^{-1}), which is normally attributed to the ATP-hydrolysis step ($k_{+3}+k_{-3}$). This was reported to be too fast to measure in the case of scS1. The similarity between values for scS1 and scHMM in the presence of calcium is in agreement with previous studies [12,14,21,22] and suggests that, in the presence of calcium, the two heads of HMM are in the on state and behave as two independent sites in binding and hydrolysing nucleotide.

The work has also shown that the binding of ATP and the ATP-hydrolysis steps are insensitive to calcium and that the heads bind and hydrolyse ATP as for scS1. It is well established that the P_i-release step, which limits the overall ATPase rate in the presence and absence of calcium, is very sensitive to calcium. This means that either the off state of scHMM binds and hydrolyses ATP as well as the on state or that the off state is formed only after ATP is hydrolysed.

The only step of the ATPase cycle involving nucleotide that is dependent on calcium is ADP release (Table 1). We demonstrate here that the affinities of ADP and mant-ADP are both 10–20-fold tighter in the absence of calcium due to a 10–20-fold reduction in the rate constant of nucleotide dissociation (k_{+6}). Both the apparent second-order rate constant of ADP association (k_{-6}/K_7) and the individual constants (K_7, k_{-6}) were independent of calcium. The second-order rate constant of ATP association (K_1k_{+2}; and the equivalent value for mant nucleotides) was also calcium-insensitive. This suggests that access to the nucleotide pocket is not affected by calcium binding to the essential light chain but that the conformation of the scHMM with bound ADP is stabilized in the absence of calcium. Furthermore, the observation that the mant-ADP dissociation rate constants measured by displacement with ADP, ATP or by eliminating mant-ADP with apyrase were identical suggests that the affinity of ADP or mant-ADP is not sensitive to the occupancy of the nucleotide pocket in the partner head of HMM.

Estimates of the affinity of ADP (and mant-ADP) for scHMM were obtained in three different ways. Analysis of the fluorescence amplitudes induced by ADP binding in Figure 2(c) (3 ± 1 and 10 ± 1 μM in the absence and presence of calcium, respectively), analysis of the amplitudes in Figures 3(c) and 3(d) (1.7 ± 0.3 and 15 ± 3 μM in the absence and presence of calcium, respectively) and from the ratio of association and dissociation rate constants (0.8–1 and 15 μM in the absence and presence of calcium, respectively). The values obtained in the absence of calcium show more variability and this is most probably due to the presence of an unregulated fraction of the HMM resulting in an overestimation of the affinity. Additionally, observations that in the absence of calcium and ADP the HMM is a mixture of the on and off states (Figure 4) may influence the estimations. In general the data are in agreement with the equilibrium estimates from Kalabokis and Szent-Györgyi [5], who had non-co-operative K_D values for ADP of 2.4 and 13 μM in the absence and presence of calcium, respectively.

The kinetics of nucleotide and calcium binding to scHMM have previously been studied by Jackson and Bagshaw [12,14]. That work used a different scallop species (*Pecten maximus*) and worked at a lower ionic strength than used here. After making allowance for these differences the two studies agree on most aspects of the work. The only major difference in the studies is that in the absence of calcium the dissociation rate constant of ADP was approx. 50 times faster in our experiments than reported by Jackson and Bagshaw [12,14]. Thus the ADP-release rate and hence the ADP equilibrium dissociation constant increased 10–30-fold in our experiments and 600-fold in the earlier study. We repeated the mant-ADP-displacement experiment in the absence of calcium at lower salt in either 10 mM Tes, pH 7.5, 1 mM $MgCl_2$ and 20 mM NaCl (the buffer used by Jackson and Bagshaw) or 20 mM Mops, pH 7.0, 5 mM $MgCl_2$ and 20 mM KCl and found essentially identical rate constants (0.01–0.03 s^{-1}) as the cited studies. This indicates that the substantial difference between the ADP-dissociation rates resolved by Jackson and Bagshaw and in this study is due to the difference in the salt concentration used in the two studies.

We were also able to estimate the calcium affinity for scHMM from the calcium dependence of the mant-ADP dissociation rate constant shown in Figure 5(b). This gave an apparent affinity of 0.78 ± 0.03 μM with a Hill coefficient of 1.9 ± 0.1. These numbers are also in close agreement with those of Kalabokis and Szent-Györgyi [5] (apparent affinity of 0.7 μM and Hill coefficient of 1.8) in the presence of ADP but significantly weaker than those in the absence of nucleotide (apparent affinity of 0.27 μM and Hill coefficient of 1.0) [5]. Our estimate of the calcium dissociation rate constant of 70 s^{-1} together with the K_D of 0.27 μM would suggest a calcium association rate constant of 2.6×10^8 $M^{-1}\cdot s^{-1}$. This value is compatible with previous estimates of calcium-binding rate constants (2.5×10^8 $M^{-1}\cdot s^{-1}$ from [12]).

The most striking observation we report here is that in the absence of calcium scHMM can only bind a single ADP, at least at ADP concentrations up to 50 μM, a concentration more than 20 times the K_D of ADP for the first site. This observation is similar to that which we made for smooth-muscle HMM, which in the absence of phosphorylation of the HMM regulatory light chains (the off state) could only bind a single ADP [16]. The observation that ATP can bind readily to the nucleotide site left vacant by ADP shows that it is not access to the site which is

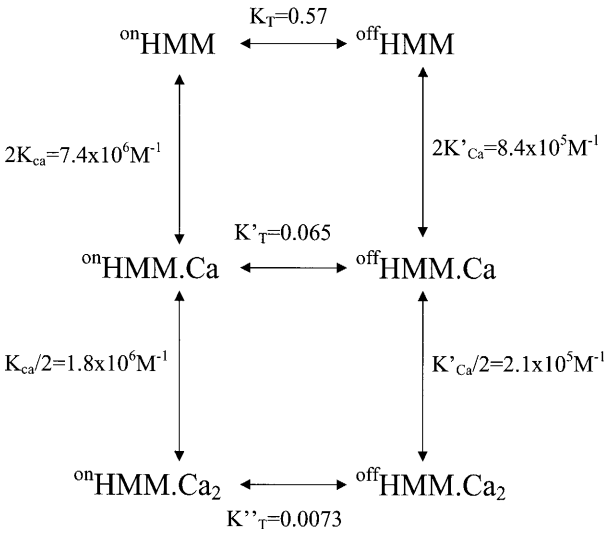

Scheme 2 Kinetic scheme for the interaction of scHMM with calcium in the absence of nucleotides

^{on}HMM and ^{off}HMM are the on and off conformations of scHMM. The equilibrium between the conformations on (^{on}HMM) and off (^{off}HMM) is defined by $K_T = [^{off}HMM]/[^{on}HMM]$ in the absence of calcium. The equilibrium constant is defined similarly when one (K'_T) or two (K''_T) calciums are bound to scHMM. K_{Ca} and K'_{Ca} are the equilibrium constants for the calcium binding to ^{on}HMM and ^{off}HMM, respectively, and 2 and 1/2 are statistical factors.

restricted but that ADP fails to form a stable complex with the empty nucleotide pocket. This is most simply explained by the ADP having insufficient binding energy to induce the correct conformation in the HMM pocket. This also requires that in the absence of calcium and presence of ADP the HMM is asymmetric, with one site having high affinity for ADP and the other low affinity.

A second unexpected result was that in the absence of calcium HMM appears to consist of two populations (in addition to the $\approx 10\,\%$ unregulated fraction). In mant-ADP-binding experiments two fractions were observed. One was characteristic of the plus-calcium form and the other one bound mant-ADP more slowly. Exact proportions of the two forms were difficult to estimate because of the different affinities of mant-ADP for the two forms and the expectation that mant-ADP binding could cause re-equilibration between the two forms. However, extrapolation to the amplitudes expected at very high [mant-ADP] suggest that approx. 30 % of scHMM was in the low-calcium off state. Thus scHMM can exist in two conformations and calcium and ADP modulate the equilibrium position between the two conformations.

A model for the regulation of scHMM

From the information gained in this study together with the work of Kalabokis and Szent-Györgyi [5] we can propose a co-operative binding model for calcium and ADP that is based on the classical Monod–Wyman–Changeux co-operative model [26] using the following observations and assumptions (see Schemes 2–4).

(i) For simplicity we assume the scHMM has two conformations, on (^{on}HMM) and off (^{off}HMM), and that both heads are either on or off. The equilibrium between the two forms is defined by $K_T = [^{off}HMM]/[^{on}HMM]$ in the absence of calcium and ADP (Scheme 2). (ii) In the presence of calcium scHMM behaves very similarly to scS1 in binding nucleotide and hydrolysing ATP. We therefore conclude that the heads are predominantly in the on state and act independently in binding nucleotide ($K''_T \ll 1$). (iii) Calcium binding to HMM in the absence of nucleotide is non-co-operative, with a K_D of 0.27 μM [5]. This defines the association equilibrium constant for calcium binding to ^{on}HMM ($K_{Ca} \approx 3.7 \times 10^6\ M^{-1}$). As the binding of calcium is non-co-operative the HMM must be predominantly in the on state in the absence of calcium and nucleotide ($K_T < 1$). Note that in the Schemes the association constant for the first site is $2 \times K_{Ca}$ and the second is $K_{Ca}/2$ for statistical reasons; there are two possible sites for the first Ca^{2+} to bind and two ways for a Ca^{2+} to leave the fully occupied HMM. (iv) In the presence of ADP calcium binding is co-operative with a 50 % saturation point of 0.8 μM and a Hill coefficient of 1.9. Assuming the simple MWC model for calcium binding shown in Scheme 2 then the association equilibrium constant for calcium binding to ^{off}HMM (K'_{Ca}) can be estimated from the $[Ca^{2+}]$ at half-saturation ($[Ca^{2+}]_m$) and K_{Ca} using $(K_{Ca} \times K'_{Ca})^{-1/2} = [Ca^{2+}]_m$ and gives a K'_{Ca} value of $4.2 \times 10^5\ M^{-1}$. (v) In the absence of both calcium and nucleotide the mant-ADP-binding experiments suggest that scHMM is in a poised equilibrium between the on and off states, with the

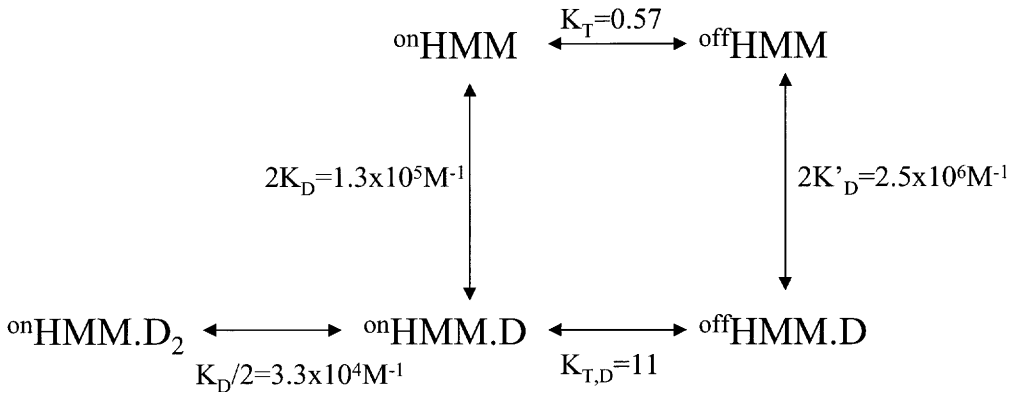

Scheme 3 Kinetic scheme for the interaction of scHMM with ADP in the absence of calcium

^{on}HMM, ^{off}HMM and K_T are the same as in Scheme 2. K_D and K'_D are the equilibrium association constants for the ADP binding to ^{on}HMM and ^{off}HMM, respectively, and 2 and 1/2 are statistical factors. The equilibrium between the on and off conformations is defined by $K_{T,D} = [^{off}HMM \cdot D]/[^{on}HMM \cdot D]$ after the binding of ADP.

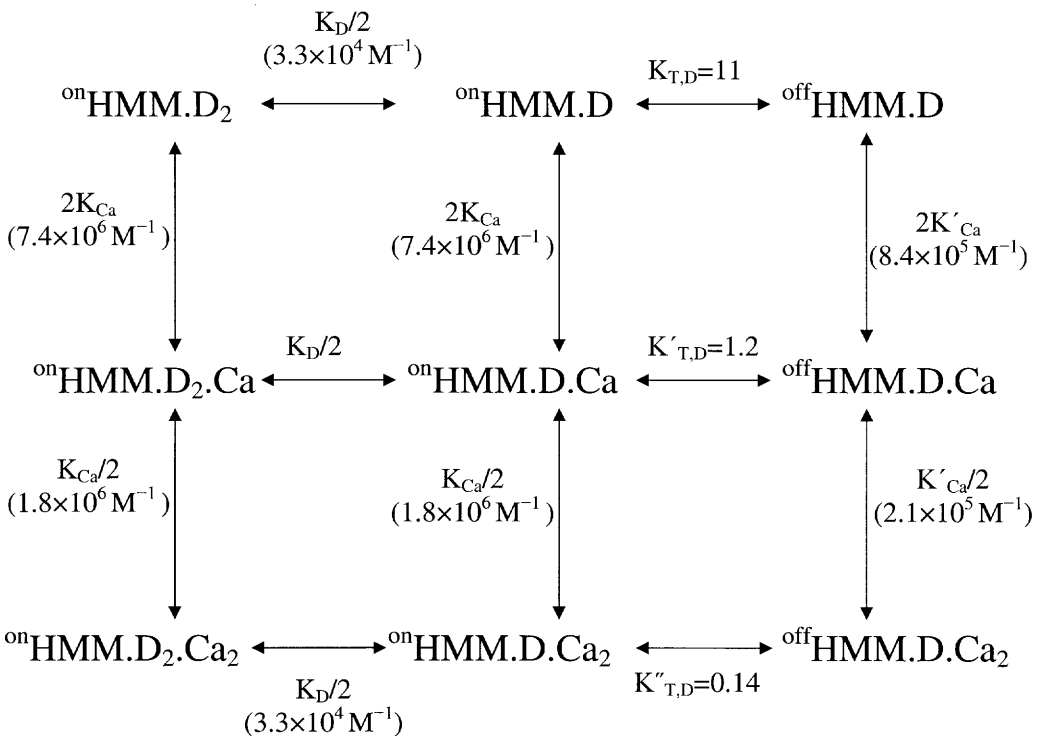

Scheme 4 Kinetic scheme for the interaction of scHMM with calcium in the presence of ADP

^{on}HMM, ^{off}HMM, K_{Ca}, K'_{Ca} and $K_{T,D}$ are the same as in Schemes 2 and 3. The equilibrium constants $K'_{T,D}$ and $K''_{T,D}$ are for the equilibrium between ^{on}HMM and ^{off}HMM conformations with one or two bound calciums, respectively.

equilibrium in favour of the on state. The ratio of the on and off forms can be estimated from the ratio of fast and slow amplitudes in mant-ADP-binding experiments. The values obtained from hyperbolae fits at saturating [mant-ADP] were 0.7:0.2 for the fast/slow components. Since the off conformation of scHMM (the slow component) can only bind one ADP (Figure 3d) the value of K_T can be calculated as $(2\times0.2)/(0.7) = 0.57$. Solving the thermodynamic box(es) in Scheme 2 then allows assignment of values for K'_T and K''_T. (vi) Equilibrium ADP binding is observed to be non-co-operative in both the presence and absence of calcium [5] with $K_D = 6.7\times10^4\ M^{-1}$ and $K'_D = 1.25\times10^6\ M^{-1}$, and ^{off}HMM binds only a single ADP (Scheme 3). K_T is defined from Scheme 2 and therefore thermodynamic balance gives $K_{T,D} = 11$. (vii) Calcium binding to HMM in the presence of ADP is shown in Scheme 4 and again thermodynamic balance allows assignment of the missing values for $K'_{T,D}$ and $K''_{T,D}$. Thus all of the equilibrium constants for the scheme can be assigned.

Implications of the model

The model can account for all of the observations reported here and those of Kalabokis and Szent-Györgyi [5]. The work suggests that in the absence of calcium and ADP the scHMM is in a poised equilibrium with approx. 30 % in the off conformation. HMM is not therefore fully in the off state unless one nucleotide pocket is occupied by ADP when it is > 90 % off. Binding of one calcium in the absence of ADP switches HMM to 5 % off and the second calcium to 0.5 % off. The binding of one calcium and one ADP gives a poised equilibrium with 55 % off and the second calcium switches the system 88 % on. The curious prediction coming from the relationships in Scheme 3 is that in the absence of calcium one ADP binding switches the system off but since the second ADP can only bind to the on state then binding of a second ADP at very high ADP concentrations should turn the system to the on state. However, consideration of the numbers in Scheme 3 suggests that this would require [ADP] > 0.5 mM to give 50 % on state and would therefore be very hard to measure. It is also well outside the physiologically relevant range of ADP concentrations.

The data presented here do not elucidate what the structures of the on and off states are, only under what conditions the two states will be occupied. The sedimentation work of Stafford et al. [18] suggests that calcium switches the scHMM between a head-up and head-down conformation but this does not explain why the nucleotide pocket does not bind ADP. Smooth-muscle myosin appears to have some similarities with the regulatory mechanism of scallop myosin and also only binds one ADP in the off state [16]. For the smooth-muscle myosin the on/off conformation involves both a 10–6 S transition involved in filament assembly and also the formation of a structure in which the two heads interact [10]. In such a structure one of the nucleotide pockets could be occluded or be trapped in a conformation with very low ADP affinity. It is known for smooth-muscle myosin S1 that ADP release from acto-S1 is coupled to a swing of the myosin neck and the associated light chains [27]. If the off structure with head–head interaction restricts movement of the HMM neck then this could result in one head having very low affinity for ADP. A similar mechanism could also operate for scHMM.

In this work we have limited ourselves to the Ca^{2+} regulation of nucleotide-binding reactions since these can be measured simply and the underlying mechanism postulated. In the case of the ATPase reaction the system is far more complicated

because the nature of the nucleotide bound to each head changes during each ATP hydrolysis cycle. We show here that the interaction between the two heads differs for empty (rigor) heads compared with heads with ADP bound at one or both sites. We also show that ATP binding to an empty head appears independent of calcium and independent of the presence of ADP on the partner head. This set of studies established that the interaction between the two heads differs for different states of the nucleotide pocket (rigor, ADP, ATP) and the nature of the interaction between the two heads may therefore also be expected to change during each ATPase cycle. The real physiological issue is the behaviour of heads with ADP and P_i bound (the steady-state complex) and these we have not yet addressed; nor have we addressed the issue of how the interaction between heads is affected by actin. These issues will be dealt with in future work.

We thank Professor Roger Goody for providing us with the mant-nucleotides and Nancy Adamek and Elisabeth O'Neall-Hennessey for technical support. This work was supported by a Wellcome Trust Programme grant 055841 and a European Union grant HPRN-CT-2000-00091 (to M.A.G.) and by a National Institutes of Health grant AR41808 (to A.G.S.-G.).

REFERENCES

1 Gordon, A. M., Homsher, E. and Regnier, M. (2000) Regulation of contraction in striated muscle. Physiol. Rev. **80**, 853–924
2 Chantler, P. D. and Szent-Györgyi, A. G. (1980) Regulatory light-chains and scallop myosin. Full dissociation, reversibility and co-operative effects. J. Mol. Biol. **138**, 473–492
3 Szent-Gyorgyi, A. G., Kalabokis, V. N. and Perreault-Micale, C. L. (1999) Regulation by molluscan myosins. Mol. Cell. Biochem. **190**, 55–62
4 Trybus, K. M. (1991) Regulation of smooth muscle myosin. Cell Motil. Cytoskel. **18**, 81–85
5 Kalabokis, V. N. and Szent-Györgyi, A. G. (1997) Cooperativity and regulation of scallop myosin and myosin fragments. Biochemistry **36**, 15834–15840
6 Xie, X., Harrison, D. H., Schlichting, I., Sweet, R. M., Kalabokis, V. N., Szent-Györgyi, A. G. and Cohen, C. (1994) Structure of the regulatory domain of scallop myosin at 2.8 A resolution. Nature (London) **368**, 306–312
7 Houdusse, A., Kalabokis, V. N., Himmel, D., Szent-Györgyi, A. G. and Cohen, C. (1999) Atomic structure of scallop myosin subfragment S1 complexed with MgADP: a novel conformation of the myosin head. Cell **97**, 459–470
8 Houdusse, A., Szent-Györgyi, A. G. and Cohen, C. (2000) Three conformational states of scallop myosin S1. Proc. Natl. Acad. Sci. U.S.A. **97**, 11238–11243
9 Offer, G. and Knight, P. (1996) The structure of the head-tail junction of the myosin molecule. J. Mol. Biol. **256**, 407–416
10 Wendt, T., Taylor, D., Trybus, K. M. and Taylor, K. (2001) Three-dimensional image reconstruction of dephosphorylated smooth muscle heavy meromyosin reveals asymmetry in the interaction between myosin heads and placement of subfragment 2. Proc. Natl. Acad. Sci. U.S.A. **98**, 4361–4366
11 Chantler, P. D., Sellers, J. R. and Szent-Györgyi, A. G. (1981) Cooperativity in scallop myosin. Biochemistry **20**, 210–216
12 Jackson, A. P. and Bagshaw, C. R. (1988) Transient-kinetic studies of the adenosine triphosphatase activity of scallop heavy meromyosin. Biochem. J. **251**, 515–526
13 Wells, C., Warriner, K. E. and Bagshaw, C. R. (1985) Fluorescence studies on the nucleotide- and Ca^{2+}-binding domains of molluscan myosin. Biochem. J. **231**, 31–38
14 Jackson, A. P. and Bagshaw, C. R. (1988) Kinetic trapping of intermediates of the scallop heavy meromyosin adenosine triphosphatase reaction revealed by formycin nucleotides. Biochem. J. **251**, 527–540
15 Kurzawa-Goertz, S. E., Perreault-Micale, C. L., Trybus, K. M., Szent-Györgyi, A. G. and Geeves, M. A. (1998) Loop I can modulate ADP affinity, ATPase activity, and motility of different scallop myosins. Transient kinetic analysis of S1 isoforms. Biochemistry **37**, 7517–7525
16 Berger, C. E., Fagnant, P. M., Heizmann, S., Trybus, K. M. and Geeves, M. A. (2001) ADP binding induces an asymmetry between the heads of unphosphorylated myosin. J. Biol. Chem. **276**, 23240–23245
17 Stafford, 3rd, W. F., Szentkiralyi, E. M. and Szent-Györgyi, A. G. (1979) Regulatory properties of single-headed fragments of scallop myosin. Biochemistry **18**, 5273–5280
18 Stafford, W. F., Jacobsen, M. P., Woodhead, J., Craig, R., O Neall-Hennessey, E. and Szent-Györgyi, A. G. (2001) Calcium-dependent structural changes in scallop heavy meromyosin. J. Mol. Biol. **307**, 137–147
19 Harrison, S. M. and Bers, D. M. (1987) The effect of temperature and ionic strength on the apparent Ca-affinity of EGTA and the analogous Ca-chelators BAPTA and dibromo-BAPTA. Biochim. Biophys. Acta **925**, 133–143
20 Bagshaw, C. R. and Trentham, D. R. (1974) The characterization of myosin-product complexes and of product-release steps during the magnesium ion-dependent adenosine triphosphatase reaction. Biochem. J. **141**, 331–349
21 Kalabokis, V. N. and Szent-Györgyi, A. G. (1998) Regulation of scallop myosin by calcium: cooperativity and the "off" state. In Mechanisms of Work Production and Work Absorption in Muscle, Advances in Experimental Medicine and Biology, vol. 453 (Sugi, H. and Pollack, G. H., eds.), pp. 235–240, Plenum Publishing, New York
22 Szent-Gyorgyi, A. G. (1996) Regulation of contraction by calcium binding myosins. Biophys. Chem. **59**, 357–363
23 Johnson, K. A. and Taylor, E. W. (1978) Intermediate states of subfragment 1 and actosubfragment 1 ATPase: reevaluation of the mechanism. Biochemistry **17**, 3432–3442
24 Millar, N. C. and Geeves, M. A. (1988) Protein fluorescence changes associated with ATP and adenosine 5′-[gamma-thio]triphosphate binding to skeletal muscle myosin subfragment 1 and actomyosin subfragment 1. Biochem. J. **249**, 735–743
25 Malnasi-Csizmadia, A., Pearson, D. S., Kovacs, M., Woolley, R. J., Geeves, M. A. and Bagshaw, C. R. (2001) Kinetic resolution of a conformational transition and the ATP hydrolysis step using relaxation methods with a *Dictyostelium* myosin II mutant containing a single tryptophan residue. Biochemistry **40**, 12727–12737
26 Monod, J., Wyman, J. and Changeux, J.-P. (1965) On the nature of allosteric transitions: a plausible model. J. Mol. Biol. **12**, 88–103
27 Whittaker, M., Wilson-Kubalek, E. M., Smith, J. E., Faust, L., Milligan, R. A. and Sweeney, H. L. (1995) A 35-A movement of smooth muscle myosin on ADP release. Nature (London) **378**, 748–751

Received 14 January 2002/13 March 2002; accepted 23 April 2002